Colloid Polym Sci 273:793–799 (1995)

ORIGINAL CONTRIBUTION

M. Maekawa
K. Murakami
H. Yoshida

Effects of type of adsorption isotherms on parallel diffusion of sulfonated dyes into porous cellulose membrane

Received: 7 December 1994
Accepted: 22 February 1995

Dr. M. Maekawa (✉) · K. Murakami
Division of Life Science and Human Technology
Nara Women's University
Nara 630, Japan

H. Yoshida
Department of Chemical Engineering
University of Osaka Prefecture
Sakai
Osaka 593, Japan

Abstract Transport phenomenon of three sulfonated azo dyes, C.I. Acid Red 88, C.I. Direct Yellow 12, and C.I. Direct Blue 15 into water-swollen cellulose membranes has been analyzed on the basis of parallel transport theory by surface and pore diffusion. Langmuir equation was applied into the mass balance equation to estimate dye concentration in the pores. The results were compared with the results obtained by applying Freundlich equation in our previous papers. The surface diffusivity (D_s) and the pore diffusivity (D_p) for the parallel diffusion model obtained by applying Langmuir equation agreed with those obtained by applying Freundlich equation. The theoretical concentration profiles for parallel diffusion calculated using D_s and D_p coincided accurately with the experimental data when we applied either Langmuir or Freundlich equations.

Key words Parallel diffusion – surface diffusion – pore diffusion – adsorption isotherm – cellulose membrane – sulfonated dye

Introduction

It is well known that dye molecules diffuse in the pores of water-swollen cellulose membrane in the kinetics of dyeing of cellulose by direct dyes [1–4]. On the other hand, intraparticle surface diffusion is well documented in the field of chemical engineering [5, 6], that is, volatile organics diffuse in the adsorbed state on the intraparticle surface of activated carbon.

In our earlier studies, we have explained the theoretical treatment for diffusion of direct dyes into the water-swollen cellulose membrane based on parallel transport by surface and pore diffusion during non-steady-state diffusion [7, 8]. Then, it was revealed that the diffusion of three sulfonated azo dyes consists of parallel diffusion with the constant pore and surface diffusivities [9–11]. As the dye concentration in the pores was assumed to be in local equilibrium with the dye concentration adsorbed on the surface of the pore wall, Freundlich equation has been applied because the adsorption of the dyes onto cellulose is described by the isotherm over a wide range of dye concentration.

In the present paper, Langmuir equation was applied in the mass balance equation and the results were compared with the results obtained by applying Freundlich equation.

Experimental

Materials

Sulfonated chromophores, C.I. Acid Red 88, C.I. Direct Yellow 12 and C.I. Direct Blue 15 shown in scheme 1 were obtained and purified as described elsewhere [9–11]. The code and molecular weight for the dyes are summarized in Table 1. The cellulose membrane (cellophane film) was

Colloid & Polymer Science, Vol. 273, No. 8 (1995)

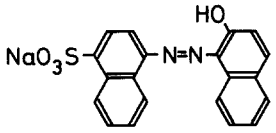

C. I. Acid Red 88

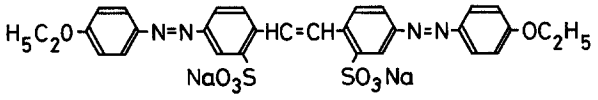

C. I. Direct Yellow 12

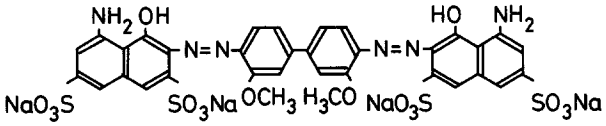

C. I. Direct Blue 15

Scheme 1 The dyes used

Table 1 The dyes and membranes used

C.I.	Dye code	M.W.	Water-swollen membrane $l(\mu m)$	ε_p	V(dm^3/kg of dry cellulose)
Acid Red 88	AR88	400.4	38.6	0.733	2.38
Direct Yellow 12	DY12	680.1	40.0	0.610	1.59
Direct Blue 15	DB15	992.8	36.4	0.757	2.65

obtained and purified as described elsewhere [7]. The thickness (l) measured by a membrane-thickness meter (Kobunshi Keiki Co., Ltd.), the void fraction (ε_p) and the volume (V) measured by the pycnometric method [8] of the water-swollen membrane were summarized in Table 1. Sodium chloride (guaranteed reagent) was obtained from Nakarai tesque and used after drying.

Diffusion of the dye – adsorption isotherms

Equilibrium isotherms were measured by batch method as described elsewhere [9–11]. Uptake curves and concentration profiles were measured by using an ultrafiltration type cell as described elsewhere [9–11]. All experiments were carried out at 55 °C. Experimental data are the same as those in our previous papers [9–11].

Theoretical

In the theoretical development of the diffusion equations, it is assumed that (1) surface and pore diffusion occur in parallel within a cellulose membrane, (2) pore and surface diffusivities are constant during the adsorption process, (3) the pore diameter and the void fraction of the membrane are constant during the adsorption process, (4) the concentration of the dye anions in the pores is in local equilibrium with the concentration of adsorbed dye anions on the surface of the pore wall, and (5) the diffusion of sodium chloride is complete before significant diffusion of the dye molecules.

These assumptions lead to the following mass balance equation:

$$\varepsilon_p \frac{\partial C}{\partial t} + \frac{\partial q}{\partial t} = \varepsilon_p D_p \frac{\partial^2 C}{\partial z^2} + D_s \frac{\partial^2 q}{\partial z^2}, \tag{1}$$

where C and q are the concentrations of the dye in the pores and on the surface of the pore wall, respectively. t and z represent time and distance through membrane. ε_p is the void fraction of the pores. D_p and D_s represent the pore and surface diffusivities, respectively. Using the dimensionless variables defined in Eq. (2), Eq. (1) can be transformed to give Eq. (3).

$$\tau_p = \frac{D_p t}{l^2}, \quad \rho = \frac{z}{l}, \quad x = \frac{C}{C_0}, \quad y = \frac{q}{q_0},$$

$$\alpha = \frac{q_0}{\varepsilon_p C_0}, \quad \beta = \alpha \frac{D_s}{D_p} \tag{2}$$

$$\frac{\partial x}{\partial \tau_p} + \alpha \frac{\partial y}{\partial \tau_p} = \frac{\partial^2 x}{\partial \rho^2} + \beta \frac{\partial^2 y}{\partial \rho^2}, \tag{3}$$

where C_0 is dye concentration in the bulk solution and q_0 is adsorbed concentration of dye in equilibrium with C_0. There are two limiting cases: $\beta = 0$ (pore diffusion control) and $\beta = \infty$ (surface diffusion control). However, Eq. (3) cannot be solved for $\beta = \infty$, and hence Eq. (1) is transformed to Eq. (4):

$$\frac{\partial x}{\partial \tau_s} + \alpha \frac{\partial y}{\partial \tau_s} = \alpha \frac{\partial^2 y}{\partial \rho^2} \quad \text{(surface diffusion control)}, \tag{4}$$

where $\tau_s = D_s t / l^2$. The relation between x and y is calculated according to the equilibrium isotherm (fourth assumption). Applying the Langmuir isotherm shown by Eq. (5), we transformed Eqs. (3) and (4) into Eqs. (6) and (7), respectively. The equilibrium constant K in Eq. (5) were evaluated from constant K_L in the Langmuir isotherm by $K = 1/(C_0 K_L + 1)$:

$$y = \frac{x}{K + (1 - K)x} \tag{5}$$

$$\left[\alpha+\frac{K}{\{1-(1-K)y\}^2}\right]\frac{\partial y}{\partial \tau_p}=K\frac{\partial}{\partial \rho}\left[\frac{1}{\{1-(1-K)y\}^2}\frac{\partial y}{\partial \rho}\right]+\beta\frac{\partial^2 y}{\partial \rho^2} \quad (6)$$

$$\left[\alpha+\frac{K}{\{1-(1-K)y\}^2}\right]\frac{\partial y}{\partial \tau_s}=\alpha\frac{\partial^2 y}{\partial \rho^2}$$

(surface diffusion control) (7)

Applying the Freundlich isotherm defined by Eq. (8), we transformed Eqs. (3) and (4) into Eqs. (9) and (10), respectively.

$$y=x^{\gamma} \quad (8)$$

$$\left[\alpha+\frac{1}{\gamma}y^{(1-\gamma)/\gamma}\right]\frac{\partial y}{\partial \tau_p}=\frac{1}{\gamma}\frac{\partial}{\partial \rho}\left[y^{(1-\gamma)/\gamma}\frac{\partial y}{\partial \rho}\right]+\beta\frac{\partial^2 y}{\partial \rho^2} \quad (9)$$

$$\left[\alpha+\frac{1}{\gamma}y^{(1-\gamma)/\gamma}\right]\frac{\partial y}{\partial \tau_s}=\alpha\frac{\partial^2 y}{\partial \rho^2} \quad \text{(surface diffusion)} \quad (10)$$

The initial and boundary conditions (I.C and B.C.) are given by Eq. (11):

$$\left.\begin{array}{l}\text{(I.C.)}\ y=0 \text{ at } \tau_p=0 \text{ or } \tau_s=0\\ \text{(B.C.)}\ y=1 \text{ at } \rho=0\ \partial y/\partial \rho=0 \text{ at } \rho=1\end{array}\right\} \quad (11)$$

Equations (6), (7), (9) and (10) were transformed into finite difference equations and solved numerically.

Results and discussion

Figure 1 shows the Langmuir plots of the equilibrium data for AR88 in the presence of different concentration of NaCl (C_E). The data correlate well with the linear lines over a wide range of dye concentration from 0.1 to 1.5 mol/m^3. On the other hand, the equilibrium isotherms for DY12 and DB15 correlated well with the equation when the dye concentration is lower than 0.3 mol/m^3, and it deviated from the isotherm at higher dye concentration where dye molecules adsorb in multilayer [8]. The equilibrium constants K in Eq. (5) are listed in Table 2. Those for DY12 and DB15 are quoted from ref. [8]. The values of α in Eq. (2) and Frendlichy constant γ taken from refs. [10–12] are also listed in Table 2. The smaller value of K and γ indicates the higher attractive force between the dye molecules and the substrate. K and γ for AR88 are larger than those for DY12 and DB15 due to lower molecular weight. The equilibrium constants, γ for Freundlich equation is independent of C_0, but the value of K decreases with increasing C_0. K is larger than γ at lower C_0, and smaller than γ at higher C_0.

Figure 2 shows the uptake curves for DB15 which shows the relation between the amount of the dye adsorbed on one sheet of cellulose membrane, $[D']$ and time (Run 20 in Table 2). The solid and broken lines represent the theoretical curves for surface and pore diffusion control, respectively. The heavy and light broken lines for pore diffusion control, respectively, show theoretical lines applied for Langmuir and Freundlich equations. The diffusivity assumed surface diffusion control, D'_s, and the diffusivity assumed pore diffusion control, D'_p, were

Fig. 1 Langmuir plot of equilibrium data for C.I. Acid Red 88 on a cellulose membrane in the presence of different concentration of NaCl at 55 °C ($0.1 \le C_0 \le 1.5$ mol/m^3). △: $C_E = 30$ mol/m^3, ○: $C_E = 50$ mol/m^3, □: $C_E = 100$ mol/m^3

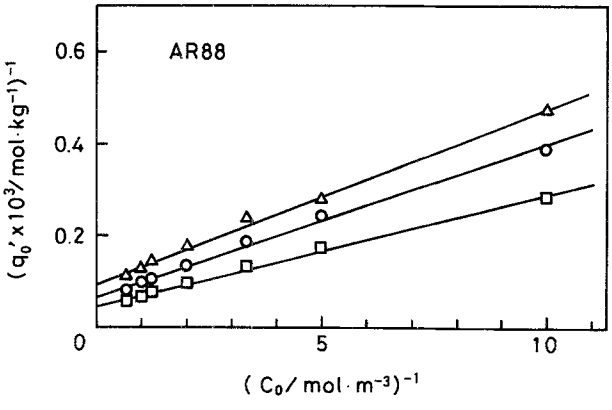

Table 2 Equilibrium constants for Langmuir and Freundlich isotherms

Run No	Dye code	C_E mol/m^3	C_0 mol/m^3	α	K	γ
1	AR88	30	0.3	7.13	0.575	0.509
2			0.5	5.57	0.448	0.509
3			1.0	4.03	0.289	0.509
4		50	0.1	14.8	0.835	0.551
5			0.3	10.1	0.627	0.551
6			0.5	7.96	0.503	0.551
7		100	0.1	20.1	0.840	0.597
8			0.2	16.6	0.724	0.597
9			0.3	14.1	0.636	0.597
10			0.5	11.8	0.512	0.597
11	DY12	30	0.1	76.8	0.522	0.424
12			0.3	40.5	0.267	0.424
13		50	0.1	109	0.503	0.441
14		100	0.1	165	0.571	0.430
15		150	0.1	209	0.541	0.473
16		250	0.1	263	0.609	0.515
17	DB15	100	0.1	152	0.260	0.230
18			0.3	60.2	0.105	0.230
19		150	0.1	199	0.232	0.219
20			0.3	80.6	0.0914	0.219
21		200	0.1	224	0.203	0.214
22			0.3	91.7	0.0784	0.214
23		250	0.1	277	0.229	0.195
24			0.3	109	0.0900	0.195

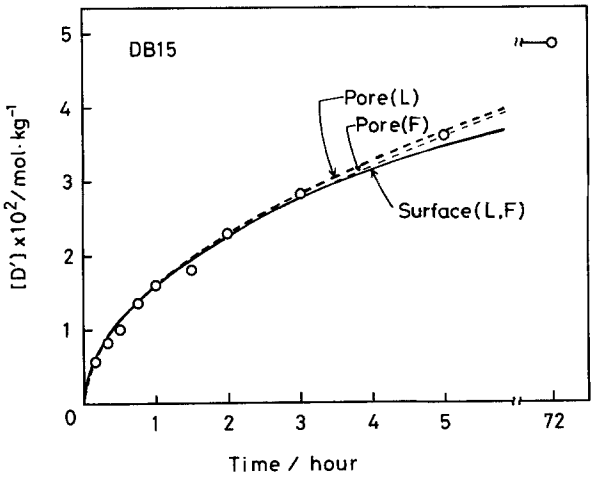

Fig. 2 Uptake curve of C.I. Direct Blue 15 on one sheet of membrane at 55 °C. Run 20, $C_0 = 0.3$ mol/m^3, $C_E = 150$ mol/m^3). The solid line represents the theoretical curve for surface diffusion applying either Langmuir or Freundlich equation ($D'_s = 3.24 \times 10^{-14}$ m^2 s^{-1}). The heavy broken line shows the theoretical line for pore diffusion applying Langmuir equation ($D'_p = 1.90 \times 10^{-12}$ m^2 s^{-1}). The light broken line shows the theoretical line for pore diffusion applying Freundlich equation ($D'_p = 1.90 \times 10^{-12}$ m^2 s^{-1})

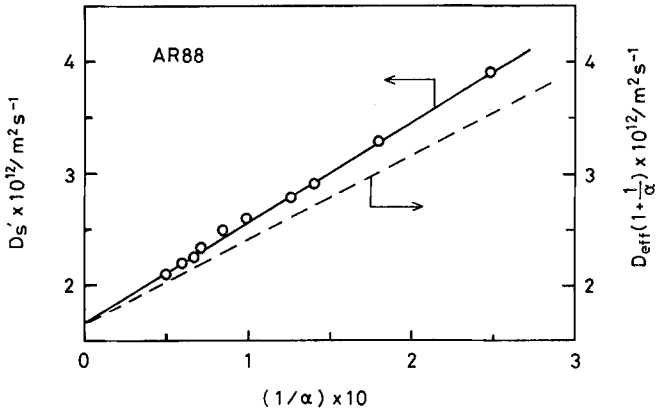

Fig. 3 Effects of α on D'_s (○) calculated from Eq. (7) by applying Langmuir equation for C.I. Acid Red 88. The solid line represents the regression line obtained from the plots of D'_s calculated from Eq. (10) by applying Freundlich equation. The broken line represents the regression line obtained from the plots for $D_{eff}(1 + 1/\alpha)$ in our previous paper [12].

obtained by matching the theoretical values calculated by using Eqs. (6), (7), (9) and (10) with the data. There is no difference between theoretical lines for surface diffusion control when applying either of these equations. On the other hand, there is a little difference between the theoretical lines for pore diffusion control when applying either Langmuir or Freundlich equation. However, the difference in D'_p is comparable to the experimental error. The values of D'_s obtained by applying Langmuir equation for AR88 are shown as a function of $1/\alpha$ in Fig. 3. They agree well with the solid line which represents the regression line for D'_s obtained by applying Freundlich equation [11]. he value of D'_s increases with decreasing α, which indicates contribution of pore diffusion is increasing with decreasing α.

In order to describe the diffusion of this system by the parallel diffusion model, we have to know the surface and pore diffusivities for the parallel diffusion. As described elsewhere [9], the effective diffusivity, D_{eff} for the homogeneous model that makes no distinction between surface and pore diffusion was calculated to determine the surface diffusivity for the parallel diffusion model according to the following procedure. Assuming Fickian diffusion with a constant effective diffusivity, the mass balance equation in the membrane is given by Eq. (12).

$$\frac{\partial [D]_L}{\partial t} = D_{eff} \frac{\partial^2 [D]_L}{\partial z^2}, \tag{12}$$

where $[D]_L$ as defined by $[D]_L = q + \varepsilon_p C$ is used.

The solution of Eq. (12) is given by Eq. (13).

$$F = 1 - 2 \sum_{n=0}^{\infty} \frac{1}{(n + 0.5)^2 \pi^2} \exp\left[-(n + 0.5)^2 \pi^2 \frac{D_{eff} t}{l^2} \right] \tag{13}$$

The value of D_{eff} were determined by matching Eq. (13) with the experimental uptake curves as shown in Fig. 2. In addition, Eq. (14) is derived from the relation between the fluxes based on the parallel diffusion and Fickian model:

$$D_{eff}\left(1 + \varepsilon_p \frac{dC}{dq}\right) = D_s + \varepsilon_p D_p \frac{dC}{dq}. \tag{14}$$

By taking C_0/q_0 for the linear isotherm system as an approximation of dC/dq, Eq. (14) is transformed into Eq. (15):

$$D_{eff}\left(1 + \frac{1}{\alpha}\right) = D_s + D_{pa} \frac{1}{\alpha}, \tag{15}$$

where D_{pa} represents the approximate pore diffusivity. The surface diffusivity for the parallel diffusion, D_s was obtained by plotting $D_{eff}(1 + 1/\alpha)$ as a function of $1/\alpha$ as the intercept of the linear line. The broken line in Fig. 3 shows the regression line for the plots of AR88 [11]. The intercept of the broken line agrees with that of solid line, though their slopes are different. Accordingly, it was appeared that we can obtain D_s by plotting D'_s as a function of $1/\alpha$ without using the homogeneous diffusion model.

The values of D'_p for DY12 were plotted as a function of α in Fig. 4. The value of D'_p increases with increasing α, which indicates the contribution of surface diffusion increases with increasing α. There is some difference between

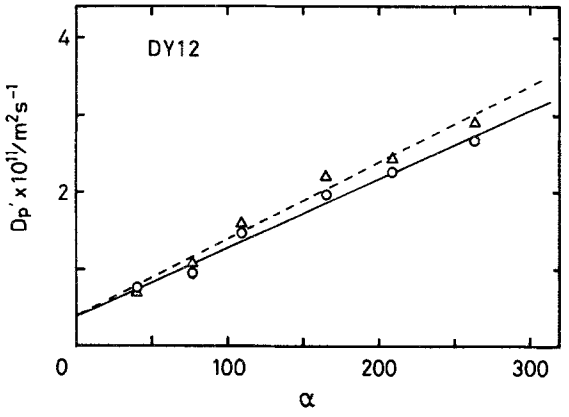

Fig. 4 Effects of α on pore diffusivity based on pore diffusion model for C.I. Direct Yellow 12. (—○—): calculated by Eq. (9) applying Freundlich equation (8), (--△--): calculated by Eq. (6) applying Langmuir equation (5)

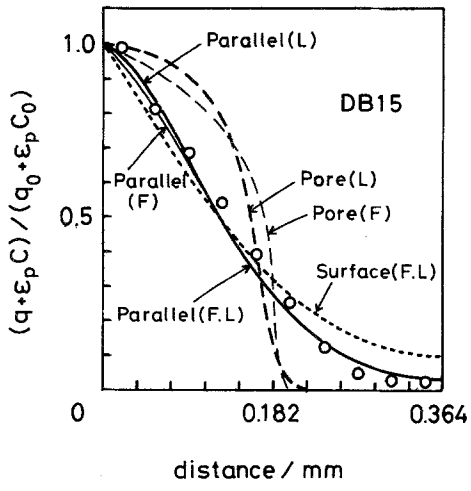

Fig. 5 The concentration profile for C.I. Direct Blue 15 in the stacked membrane at 55 °C for 144 h diffusion time (see Run 22 in Table 2); (---): surface diffusion control ($D_s' = 3.27 \times 10^{-14}$ m^2 s^{-1}), (– – –): pore diffusion control applying Langmuir equation ($D_p' = 2.15 \times 10^{-12}$ m^2 s^{-1}), (– · –): pore diffusion control applying Freundlich equation ($D_p' = 2.27 \times 10^{-12}$ m^{2}s^{-1}), (—): parallel diffusion model applying Langmuir equation ($D_s = 2.05 \times 10^{-14}$ m^2 s^{-1} and $D_p = 5.13 \times 10^{-13}$ m^2 s^{-1}), (—): parallel diffusion model applying Freundlich equation ($D_s = 2.05 \times 10^{-14}$ m^2 s^{-1} and $D_p = 5.13 \times 10^{-13}$ m^2 s^{-1})

Table 3 The surface diffusivities and the pore diffusivities for the parallel diffusion model of three dyes

dye	D_s/m^2 s^{-1}	D_p/m^2 s^{-1}
C.I. Acid Red 88	1.66×10^{-12}	4.77×10^{-12}
C.I. Direct Yellow 12	1.18×10^{-13}	3.59×10^{-12}
C.I. Direct Blue 15	2.05×10^{-14}	5.13×10^{-13}

values obtained by applying Langmuir or Freundlich isotherm, however, the intercepts of the lines agreed. The intercept provides the pore diffusivity for the parallel diffusion, D_p as described earlier [10]. The values of D_s and D_p of three dyes were summarized in Table 3.

Figures 5 and 6 show the experimental concentration profiles of DB15 (Run 22 in Table 2) and DY12 (Run 11 in Table 2) obtained from a stack of 10 sheets of the membrane. The period of the contacting time with the solution was 144 h for DB15 and 24 h for DY12. The long-dashed lines, the short-dashed line and the solid lines show the theoretical lines for pore diffusion control, surface diffusion control and parallel diffusion, respectively. The light and heavy lines, respectively, show the theoretical lines obtained by applying Freundlich and Langmuir equations. The theoretical lines for surface diffusion control are not affected by the type of the isotherm, however, those for pore diffusion control are affected by the applied equation. As described elsewhere [7, 8] concentration profiles are affected by the equilibrium constant. The concentration near the membrane surface is higher and the profile is steeper for smaller equilibrium constants than that for larger ones. Accordingly, the theoretical line for pore diffusion applied Langmuir equation ($K = 0.0748$) is steeper than that applied Freundlich equation ($\gamma = 0.214$) in Fig. 5. When equilibrium constant increases, the slope becomes gentle, resulting in the difference between the theoretical profile for surface diffusion control and for pore diffusion control becoming small, as is clear for that of DY12 in Fig. 6 ($K = 0.522$ and $\gamma = 0.424$).

As described elsewhere [7, 8, 11], an indicator of the type of controlling diffusion is β ($= \alpha D_s/D_p$). Diffusion can be approximated by pore diffusion when $\beta \leqq 0.1$ and by surface diffusion when $\beta \geqq 1.0$. Parallel diffusion occurs for $0.1 < \beta < 10$. As β for Runs 22 and 11 are 3.66 and 2.52, respectively, the theoretical lines for parallel diffusion were calculated by using D_s and D_p in Table 3. Actually, the theoretical concentration profile for parallel diffusion calculated by applying Langmuir equation differs somewhat from that applying Freundlich isotherm, however, both of them agree well with the experimental data within the experimental error.

Figure 7 shows the experimental concentration profile of AR88 with largest equilibrium constant ($K = 0.840$, Run 7 in Table 2). The period of the contacting time with the solution was 2 h. The long-dashed lines, the short-dashed line, and the solid lines in the figure show the theoretical lines for surface diffusion control, pore diffusion control and parallel diffusion calculated by applying Langmuir equation, respectively. The theoretical line for parallel diffusion agree best with the experimental data, however, not only the theoretical line for surface diffusion

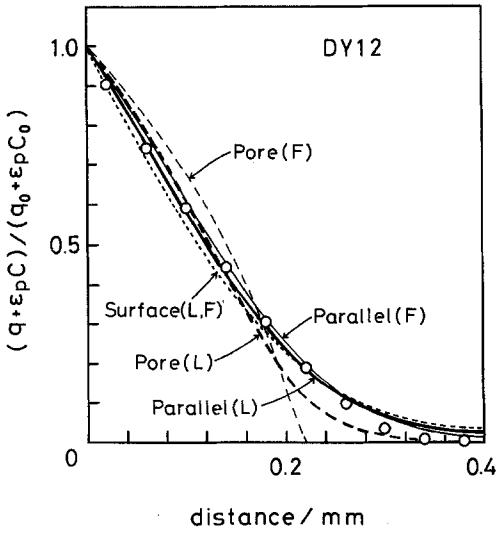

Fig. 6 The concentration profile of C.I. Direct Yellow 12 in the stacked membrane at 55 °C for 24 h diffusion time (see Run 11 in Table 2); (---): surface diffusion control ($D'_s = 1.62 \times 10^{-13}$ m^2 s^{-1}), (–––); pore diffusion control applying Langmuir equation ($D'_p = 9.66 \times 10^{-12}$ m^2 s^{-1}), (– – –): pore diffusion control applying Freundlich equation ($D'_p = 9.41 \times 10^{-12}$ m^2 s^{-1}), (—): parallel diffusion model applying Langmuir equation ($D_s = 1.18 \times 10^{-13}$ m^2 s^{-1} and $D_p = 3.59 \times 10^{-12}$ m^2 s^{-1}), (—): parallel diffusion model applying Freundlich equation ($D_s = 1.18 \times 10^{-13}$ and $D_p = 3.59 \times 10^{-12}$ s^{-1})

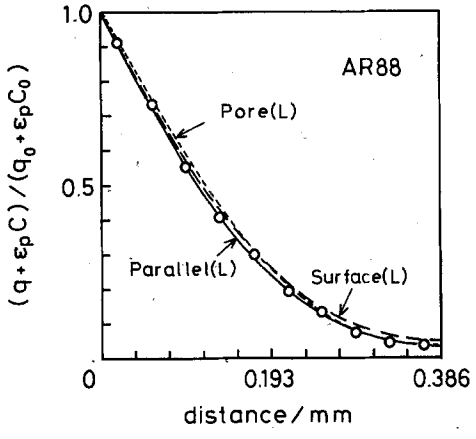

Fig. 7 The concentration profile of C.I. Acid Red 88 in the stacked membrane at 55 °C for 2 h diffusion time (see Run 7 in Table 2); (– – –): surface diffusion control applied Langmuir equation ($D'_s = 2.10 \times 10^{-12}$ m^2 s^{-1}), (---): pore diffusion control applying Langmuir equation ($D'_p = 4.05 \times 10^{-11}$ m^2 s^{-1}), (—): parallel diffusion model applying Langmuir equation ($D_s = 1.66 \times 10^{-12}$ m^2 s^{-1} and $D_p = 4.77 \times 10^{-12}$ m^2 s^{-1})

control, but also that for pore diffusion control agree well with the experimental data despite large β (= 6.99) where the contribution of surface diffusion is large. As described elsewhere [11], the diffusion behavior of AR88 is specific

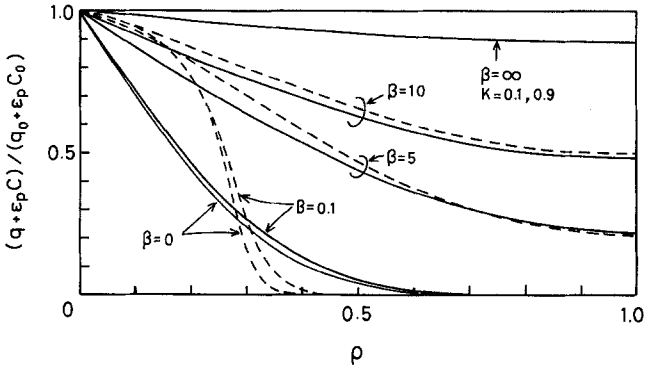

Fig. 8 Effects of K and β on the concentration profiles when Langmuir equation is applied. $\alpha = 30$, $\tau = 1$. (—): $K = 0.9$, (– – –): $K = 0.1$

because of strong tendency to aggregate in the liquid phase [12, 13]. The dye molecules diffuse on the surface of pore wall as a monomer and in the liquid phase in pores as a mixture of monomer and dimer, resulting that β becomes large due to smaller D_p. Figure 7 suggests that the type of controlling diffusion cannot be judged from the concentration profile when equilibrium constant is large. Figure 8 represents the effects of K on the concentration profiles at various β. When $K = 0.1$, the profiles of surface diffusion control ($\beta \geqq 10$) differ from those of pore diffusion control ($\beta \leqq 0.1$), where the dye concentrations near the membrane surface are high and then slopes become steep. On the other hand, the slopes of the profiles are gentle without depending on β when $K = 0.9$. The equilibrium constant, K of Run 7 is so large as 0.840 that the theoretical profile for surface and pore diffusion control became similar.

Conclusions

Uptake curves and concentration profiles for AR88, DY12 and DB15 in a cellulose membrane were analyzed based on the parallel surface and pore diffusion theory. Langmuir equation was applied in the mass balance equation to estimate dye concentration in the pores. The results were compared with those applying Freundlich equation. The following conclusions were made. 1) The surface and pore diffusivities for the parallel diffusion coincided when applying either Freundlich and Langmuir equations. 2) The theoretical concentration profiles for parallel diffusion calculated using obtained D_s and D_p agreed well with the experimental data when applying either of these equations. 3) The validity of the theory to obtain the dye concentration in the pores from the equilibrium isotherm and to describe the diffusion of these dyes by the parallel diffusion model was confirmed.

References

1. McGregor R, Peters RH, Petropolous JH (1962) Trans Faraday Soc 58:1045
2. Warwicker JO (1963) J Polym Sci Part A 1:3105
3. Hori T, Mizuno M, Shimizu T (1980) Colloid Polym Sci 258:1070
4. Morita Z, Tanaka T, Motomura H (1986) J Appl Polym Sci 31:777
5. Suzuki M, Kawazoe K (1975) J Chem Eng Japan 8:379
6. Suzuki M, Kawai T, Kawazoe K (1976) J Chem Eng Japan 9:203
7. Yoshida H, Kataoka T, Nango M, Ohta S, Kuroki N, Maekawa M (1986) J Appl Polym Sci 32:4185
8. Yoshida H, Kataoka T, Maekawa M, Nango M (1989) Chemical Eng J 41:B1
9. Yoshida H, Maekawa M, Nango M (1991) Chemical Eng Sci 46:429
10. Maekawa M, Murakami K, Yoshida H (1993) J Colloid Interface Sci 155:79
11. Maekawa M, Tanaka M, Yoshida H (1995) J Colloid Interface Sci 170:146
12. Hamada K, Nonogaki H, Fukushima Y, Munkhbat B, Mitsuishi M (1991) Dyes Pigm 16:111
13. Hamada K, Mitsuishi M (1992) Dyes Pigm 19:161